Recurrence and Photon Statistics in Fluorescence Fluctuation Spectroscopy

Gert Zumofen,[1] Johannes Hohlbein,[2,3] and Christian G. Hübner[2,*]

[1]*Swiss Federal Institute of Technology, Physical Chemistry, CH-8093 Zurich, Switzerland*
[2]*Physics Department, University Halle, Hoher Weg 8, D-06099 Halle, Germany*
[3]*Max Planck Institute of Microstructure Physics, Weinberg 2, D-06120 Halle, Germany*

(Received 20 August 2004; published 20 December 2004)

We report on fluorescence fluctuations of nanoparticles diffusing through a laser focus. Subject to an intensity threshold the fluorescence signal is transformed into time traces of on and off periods. The distribution functions of the experimental on and off times follow power laws $t^{-\alpha}$ over several orders of magnitude with exponents $\alpha \simeq 1.5 - 2$. At long times the distribution functions cross over to exponential decays. For the interpretation of the experimental data a diffusion-reaction equation is proposed which covers both, the diffusion controlled recurrence and the photon statistics as the relevant processes.

DOI: 10.1103/PhysRevLett.93.260601 PACS numbers: 05.40.Jc, 82.37.–j, 87.64.Tt

Confocal detection of the fluorescence originating from single molecules or nanoparticles diffusing freely in solution has attracted much attention in various fields of life sciences [1–5]. The particular charm of this method lies in its capability to study processes in living cells under close to physiological conditions [6]. Briefly, a microscope objective is used both for diffraction-limited focussing of laser light onto the sample and for collection of the emitted light from the focal region thus defining a confocal volume from where particles' fluorescence is detected. Several methodologies have been developed for the fluorescence data analysis, of which the fluorescence correlation spectroscopy (FCS) [4], the fluorescence intensity distribution analysis (FIDA) [7], and the fluorescence burst size distribution analysis (BSDA) [8] are the most widely employed techniques. For the identification of individual fluorescence bursts and the recognition of single molecules in the detection volume an intensity-threshold criterion is usually introduced [9]. Prominent problems encountered in this type of analysis are the assignment of consecutive bursts to the same molecule reentering or to a different molecule entering the focal volume and the uncertainty imposed by the photon statistics.

In this Letter we report on nanometer sized fluorescent spheres diffusing freely through a laser focal volume. Upon a threshold number θ of photons, probability distribution functions (PDFs) of on and off periods are determined. It is shown that diffusion and photon statistics are essential for the description of the observations and that a diffusion-reaction equation allows for the discussion of all the features observed in the on and off PDFs. Thus the present investigation is concerned with a classical problem of diffusion, namely, the probabilities of freely diffusing particles to escape from the area of initialization and of crossing boundaries for the first time, i.e., first-passage events [10,11].

For the experiment, yellow fluorescent latex spheres of 32–200 nm diameter (Sigma-Aldrich) were suspended in water at concentrations equivalent to $\simeq 10^{-11}$ M. A homemade scanning confocal optical microscope was applied with a $\lambda = 488$ nm solid state laser as the excitation source and single photon counting avalanche photodiodes (SPADs, SPCM AQ-14, Perkin-Elmer) as detectors featuring a dark count rate of 100 s^{-1}. An oil-immersion microscope objective (Apochromat 100×1.4, Nikon) was used for both diffraction-limited focusing of the light and collection of the fluorescence. The laser intensity was typically between 5 and 300 nW thus avoiding saturation effects as well as biased diffusion due to restoring forces. Transient intensities were recorded by collecting photons in bins of $\tau = 100$ μs width. For several threshold values θ the transient intensities were translated into binary time traces of on and off periods. An example of the transient intensity trace is shown in Fig. 1 on different time scales together with the on and off periods in a bar-code–like style. The patterns of the on and off periods show a self-similar structure indicating a pronounced scaling behavior of the on and off periods.

The binary time traces were then used to determine PDFs of the on and off times. Examples of PDFs are given in Fig. 2. By inspection of these PDFs, one notices three different time regimes. At short times there is a transition from a flat to a power-law regime governed primarily by an exponent $\alpha = 3/2$ for off and $\alpha \simeq 2$ for on times. At long times the data indicate transitions to exponential decays where with increasing θ the onset of the exponentials occur at shorter and longer times for on and off states, respectively. Surprisingly, clear deviations in the short time regime between the on- and off-PDFs for small thresholds θ are visible that almost vanish with increasing θ.

Our model is based on particles diffusing freely through the confocal volume. We define a space dependent instrument response function (IRF) $\Lambda(\mathbf{r})$, which denotes the average number of photons per bin time detected for a stationary particle located at position $\mathbf{r}$. $\Lambda(\mathbf{r})$ thus results from the collective fluorescence of the bead's chromophores and from the collection-efficiency function [1]. Depending on the setup $\Lambda(\mathbf{r})$ shows characteristic shapes with primarily Gaussian form in the focal plane and power law form in the axial direction with oscillations super-

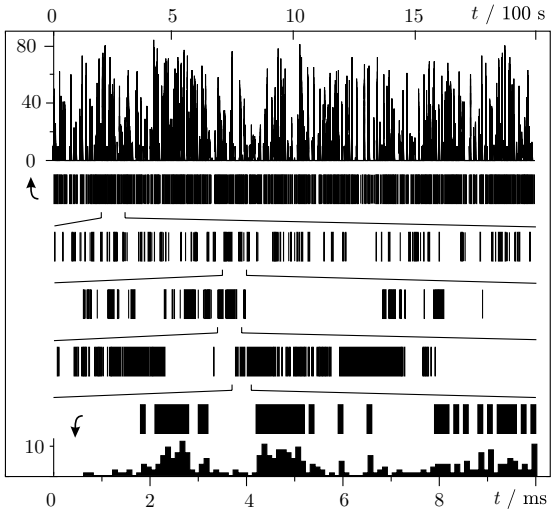

FIG. 1. Experimental intensity time traces and on and off periods of 200 nm beads. Intensities are given in units of photon counts. On the intermediate panels the on periods are given by black bars for $\theta = 3$ on consecutively zoomed-in scales with magnification factors of approximately 20. The top two and the lowest two panels refer to the top and bottom time scale, respectively.

imposed. We assume an identical shape for the laser-intensity and collection-efficiency function for the confocal setup and write for the IRF in cylinder coordinates (ρ, z)

$$\Lambda(\rho, z) = \Lambda_0\left[\frac{w_0^2}{w^2(z)}\exp\left(\frac{-2\rho^2}{w^2(z)}\right)\right]^2, \tag{1}$$

where Λ_0 is the number of photons per bin for a particle at the center and w stands for the z-dependent focal waist

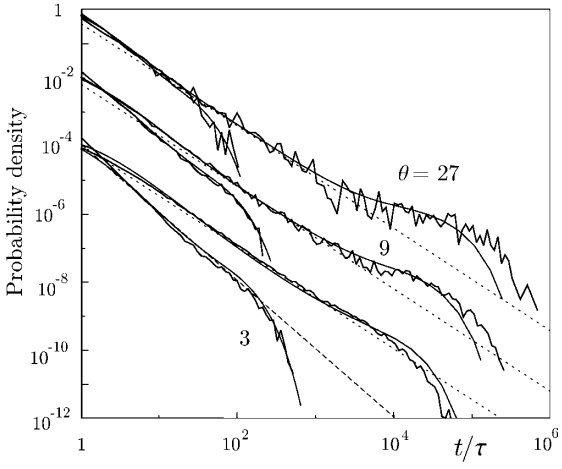

FIG. 2. Experimental and calculated on and off PDFs. Pairs of curves give on PDFs (lower line) and off PDFs (upper line) for thresholds θ, as indicated, and are shifted vertically for clarity. The wiggly lines give the experimental data of Fig. 1 and the smooth lines are the calculations. Dotted and dashed lines are power laws with exponents $\alpha = 3/2$ and 2, respectively.

$w^2(z) = w_0^2[1 + (z/z_0)^2]$. The ratio z_0/w_0 was determined by direct measurement of the focal IRF yielding $z_0/w_0 \simeq 3/2$ which corresponds to a geometrical length to width ratio of $\simeq 3$, visible in Fig. 4. Based on Poissonian statistics the probability of n photons per bin is $U(n, \mathbf{r}) = e^{-\Lambda}\Lambda^n/n!$ of a particle located at $\mathbf{r}$. Subject to θ we denote by $p_-(\mathbf{r}; \theta)$ the off-state probability with $n \leq \theta$

$$p_-(\mathbf{r}; \theta) = \sum_{n=0}^{\theta} U(n, \mathbf{r}). \tag{2}$$

The complementary probability $p_+ = 1 - p_-$ then denotes the on-state probability with $n > \theta$. Here and in the following we denote by the subscripts $+$ and $-$ the on and off states. We next define the probability of an interval for N consecutive bins of on state, $\psi_+(N) = p_-(\mathbf{r}_0) \times p_+(\mathbf{r}_1)\cdots p_+(\mathbf{r}_N)p_-(\mathbf{r}_{N+1})$, which depends on the particular realization of the diffusion path with positions $\mathbf{r}_0, \mathbf{r}_1, \mathbf{r}_2, \cdots$ at times $t_0 = 0, t_1 = \tau, t_2 = 2\tau, \cdots$. Averaging over all possible realizations of the diffusion path leads to the space averaged probability density of on periods

$$\langle\psi_+(t)\rangle = \tau^{-1}\langle p_-(\mathbf{r}_0)p_+(\mathbf{r}_1)\cdots p_+(\mathbf{r}_N)p_-(\mathbf{r}_{N+1})\rangle, \tag{3}$$

where the time is discretized according to $t = N\tau$ and where an appropriate normalization is taken into account. $\langle\psi_+(t)\rangle$ is thus the probability density for the on state to end in the interval $[t, t + dt]$. The derivation of the off probabilities $\langle\psi_-(t)\rangle$ follows from the same reasoning by simply interchanging the subscripts $-$ and $+$. The description of Eqs. (2) and (3) can be generalized to several particles in a given volume and straightforward calculations can be carried out using Monte Carlo simulation. However, it is not obvious, how to derive analytical expressions for the on and off PDFs. We therefore restrict the approach assuming that the concentration is small so that to a good approximation there is only one particle in the focal volume. Within this model assumption we consider first two limiting cases: strong fluorescence and slow diffusion, and then propose a diffusion-reaction equation for the general case.

In the limit of strong fluorescence we assume that the recorded photon stream is so strong that photon shot noise is negligible. Accordingly, the border of probability where the diffusing particle changes state from on to off and vice versa becomes sharp. The task is thus transformed into a first-passage problem for particles to reach a boundary for the first time. The particles are initiated close to the boundary, either inside for on or outside for off states, respectively. First-passage probabilities are calculated from the PDFs $P_\pm(\mathbf{r}, t)$ which obey the diffusion equation subject to an absorbing boundary [10]. For the spherical symmetric case

$$\partial_t P_\pm(r, t) = Dr^{-2}\partial_r r^2 \partial_r P_\pm(r, t), \tag{4}$$

$$P_\pm(r, 0) = \delta(r - r_0)/(4\pi r_0^2), \qquad P_\pm(r_a, t) = 0, \tag{5}$$

where r_a denotes the radius of the absorbing boundary. The small initial displacement $\Delta = |r_0 - r_a|$ we set equal to the spatial resolution given by the diffusion length within the bin time, $\Delta^2 = 2D\tau$. From $P_\pm(\mathbf{r}, t)$ we calculate the corresponding survival probabilities $S_\pm(t)$ and the first-passage density $\langle\psi_+(t)\rangle$ according to

$$S_\pm(t) = 4\pi \int_0^\infty P_\pm(r, t) r^2 dr, \qquad \langle\psi_+(t)\rangle = -dS_+/dt. \tag{6}$$

While the on states are limited by the outer absorbing boundary the particles initiated outside of the absorbing boundary may escape to infinity with probability equal to Δ/r_0 [10]. The off times are thus eventually limited by the arrival of other *bulk* particles. Within the model of a discrete absorbing boundary we provide an accurate description of the survival probability subject to the joint arrival of a particle initiated close to the surface and bulk particles. We take into account the independence of particles and write for the survival probability S_- that no particle has reached the boundary by time t and corresponding first-passage density

$$S_- = S_- S_b, \qquad \langle\psi_-\rangle = -dS_-/dt. \tag{7}$$

Here S_b refers to the bulk particles. From a stationary approach one may see that the initial condition for the spatial density $C(r, 0)$ of bulk particles is homogeneous at the instance when the last particle leaves the focal area. Therefore, making use of the Green's function approach, the evolution of the bulk particle density is

$$C(r, t) = 4\pi c_0 \int_{r_b}^\infty P(r, t|r_0) r_0^2 dr_0, \tag{8}$$

where c_0 is the particle concentration and r_b denotes the onset radius of bulk particles and may be equated with r_0 or r_a. According to Smoluchovski [12] the rate $k(t)$ of the particles' arrival and corresponding survival is

$$k(t) = 4\pi D r_a^2 \partial_r C(r, t)|_{r_a}, \qquad S_b = e^{-\int_0^t k(t)dt}. \tag{9}$$

Using the techniques developed for heat conduction [13] all the required quantities can be given as series of elementary functions. For short times the leading term reads

$$\langle\psi_\pm\rangle \sim t^{-3/2} e^{-(\tau/2t)} \tag{10}$$

and for long times

$$\langle\psi_+\rangle \sim e^{-(\pi^2 Dt/r_a^2)}, \qquad \langle\psi_-\rangle \sim t^{-1/2} e^{-4\pi c_0 r_a Dt}. \tag{11}$$

The calculated PDFs in Fig. 3(a) show three regimes. At short times, the behavior is governed by an increase resulting from the time required for the particle to approach the boundary. The second regime shows a power-law behavior with exponent $\alpha = 3/2$, which manifests the typical return PDF in 3D [10]. The long-time behavior is governed by exponentials because of the finite volume imposed by the absorbing boundary for on states and because bulk particles reach the absorbing boundary for off states. We note the characteristic transition from the power law to the exponential decay which is different for on and off states. We further note that Fig. 3(a) captures already the majority of the features observed experimentally in Fig. 2, namely, the crossover at short times, the intermediate power law and the exponential at long times. However, contrary to the observations, the on and off PDFs show identical patterns except for the exponentials at long times.

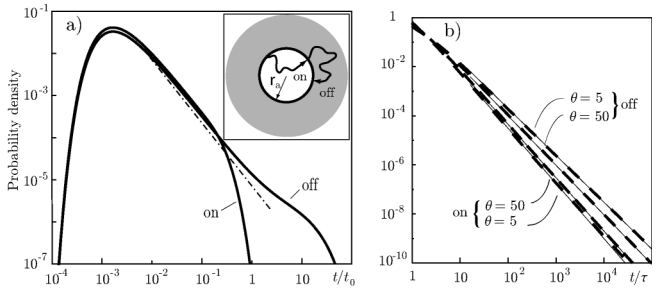

FIG. 3. First-passage PDFs for two limiting cases. (a) $\langle\psi_\pm(t)\rangle$ of Eqs. (6) and (7) based exclusively on diffusion. The ratio of the initial displacement and the radius of the absorbing sphere is $\Delta{:}r_a = 1{:}10$ and the particle density is given by $4\pi c_0 r_a^3/3 = 0.02$. Time t is given in units of $t_0 = r_a^2/D$. The dash-dotted line is a power law with exponent $\alpha = 3/2$. The inset illustrates a diffusion path and first passages in 2D with a permeable circle. The shaded area indicates the homogeneous initial density $C(r, 0)$ of bulk particles. (b) $\langle\psi_\pm(t)\rangle$ based exclusively on photon statistics. Calculations of Eq. (12) are given by dashed lines for $\Lambda_0 = 100$ and for θ values, as indicated. The thin lines indicate power laws $t^{-\alpha}$ from bottom to top with exponents: 2.25, 2.15, 2.0, 1.9.

We next consider the slow diffusion limit where we assume that the time of crossing the focal volume is much larger than the time scale of $\langle\psi_\pm(t)\rangle$. In this case the average in Eq. (3) reads

$$\langle\psi_\pm(t)\rangle = \tau^{-1}\langle p_\mp^2(\mathbf{r}) p_\pm^N(\mathbf{r})\rangle, \qquad N = t/\tau. \tag{12}$$

Numerical calculations were carried out for $\Lambda(\mathbf{r})$ of Eq. (1) and results of the PDFs are shown in Fig. 3(b). Power laws fitted to the numerical PDFs yield exponents of $\alpha \simeq 2$. From a rough analysis of the asymptotic behavior the estimated decay follows a power law with exponent $\alpha = 2$ and with logarithmic corrections. We notice that, contrary to the diffusion controlled PDFs in Fig. 3(a), here the PDFs of the on and off states differ from each other. Similar deviations arise also for spherical quadratic Lorentzian $\Lambda(\mathbf{r})$, however, the deviations are much smaller for pure Gaussian $\Lambda(\mathbf{r})$. Thus deviations result from the asymmetry imposed on the p_- and p_+ functions subject to a mirror placed tangentially at the maximum location of $p_- p_+$.

Motivated by the above analysis we propose the following diffusion-reaction equation for the general case still assuming small concentrations so that primarily only one

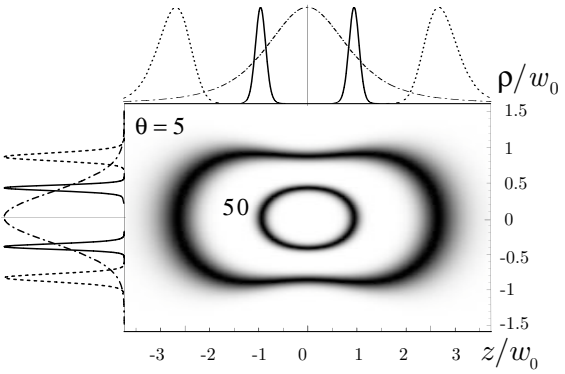

FIG. 4. Change of state probabilities $p_- p_+$ in the focal zone for $\Lambda(\rho, z)$ of Eq. (1) and for $\Lambda_0 = 100$ and $z_0/w_0 = 3/2$. The outer and the inner shaded area result from thresholds θ as indicated. On the left and top the full and dashed lines denote the probabilities $p_- p_+$ in the focal plane and along the z axis, respectively. The transverse and longitudinal IRFs $\Lambda(\rho, 0)$ and $\Lambda(0, z)$ are given by dash-dotted lines.

particle is in the focus

$$\partial_t P_\pm(\mathbf{r}, t) = [D\nabla^2 - K_\pm(\mathbf{r})]P_\pm(\mathbf{r}, t). \tag{13}$$

We equate the initial condition for single particles $P_\pm(\mathbf{r}, 0)$ with the stationary state probability of the particle to change state at location $\mathbf{r}$. Similarly, we propose that the bulk density $C(\mathbf{r}, t)$ obeys Eq. (13) for the minus state subject to homogeneous initial conditions limited by $p_-(\mathbf{r})$, so that

$$P_\pm(\mathbf{r}, 0) = \mathcal{N} p_-(\mathbf{r}) p_+(\mathbf{r}), \qquad C(\mathbf{r}, 0) = c_0 p_-(\mathbf{r}), \tag{14}$$

where $\mathcal{N}$ accounts for normalization. Similarly, we equate the space dependent reaction rate $K_\pm(\mathbf{r})$ with the probability of the particle located at $\mathbf{r}$ to generate a number of photons which overcomes the θ criterion of changing state

$$K_\pm(\mathbf{r}) = -\tau^{-1} \ln p_\pm(\mathbf{r}). \tag{15}$$

We notice that in the limit of strong fluorescence, $K_\pm$ converges to a step function so that the first-passage problem is recovered. In the limit of slow diffusion the diffusion term in Eq. (13) can be dropped and taking Eq. (6) into consideration one can show that Eqs. (12) and (13) are compatible. The survival is calculated according to Eq. (6) and the rate of bulk arrival is $k(t) = \int K_-(\mathbf{r}) C(\mathbf{r}, t) d\mathbf{r}$.

In Fig. 4 the initial conditions $p_- p_+$ are displayed. A pronounced asymmetry is clearly visible for $\theta = 5$. Calculated PDFs are shown in Fig. 2 for the parameters $w_0^2/D\tau = 670$ and $c_0 w_0^3 = 1.5 \times 10^{-3}$ estimated independently from FCS and $\Lambda_0 = 60$ from FIDA, respectively. The calculations are in good agreement with the observations, particularly, the deviations between the on and off PDFs are well reproduced. The residual deviations between calculation and experiment turned out to depend sensitively on the shape of the IRF.

In conclusion, we have shown that on and off PDFs provide a powerful tool for the investigation of recurrence in fluorescence fluctuation spectroscopy. The proposed diffusion-reaction equation provides an accurate description of the PDFs taking into account diffusion and photon statistics on equal footing and including the multiple particle problem for off states. Contrary to FCS, the present method is sensitive to the focal shape. Deviations between the on and off PDFs result primarily from the non-Gaussian shape of the IRF. We expect that the experimental restriction of the diffusion to 1D or 2D would allow us to study the dimensionality dependence of the recurrence.

We thank T. Aumüller, J. Klafter, A. Renn, V. Sandoghdar, and J. Seelig for stimulating discussions.

*Electronic address: ch.huebner@physik.uni-halle.de

[1] *Single Molecule Detection in Solution*, edited by C. Zander, J. Enderlein, and R. A. Keller (Wiley-VCH, Weinheim, 2002).
[2] A. A. Deniz *et al.*, Annu. Rev. Phys. Chem. **52**, 233 (2001).
[3] D. Magde *et al.*, Phys. Rev. Lett. **29**, 705 (1972).
[4] M. Eigen and R. Rigler, Proc. Natl. Acad. Sci. U.S.A. **91**, 5740 (1994).
[5] S. Nie, D. T. Chiu, and R. N. Zare, Science **266**, 1018 (1994).
[6] K. M Berland *et al.*, Biophys. J. **68**, 694 (1995).
[7] Y. Chen *et al.*, Biophys. J. **77**, 553 (1999).
[8] J. Enderlein, D. I. Robbins, W. P. Ambrose, and R. A. Keller, J. Phys. Chem. A **102**, 6089 (1998).
[9] C. Eggeling *et al.*, Proc. Natl. Acad. Sci. U.S.A. **95**, 1556 (1998); A. A. Deniz *et al.*, Proc. Natl. Acad. Sci. U.S.A. **96**, 3670 (1999); B. Schuler , E. A. Lipman, and W. A. Eaton, Nature (London) **419**, 743 (2002).
[10] S. Redner, *A Guide to First-Passages Processes* (Clarendon Press, Oxford, 2003).
[11] G. H. Weiss, *Aspects and Applications of the Random Walk* (North Holland, Amsterdam, 1994).
[12] M. von Smoluchovski, Z. Phys. Chem. **92**, 129 (1917).
[13] H. S. Carslaw and J. C. Jaeger, *Conduction of Heat in Solids* (Clarendon Press, Oxford, 2003).